

Wit GRZESIK
Piotr NIEŚŁONY
Witold HABRAT

INVESTIGATION OF THE TRIBOLOGICAL PERFORMANCE OF AlTiN COATED CUTTING TOOLS IN THE MACHINING OF Ti6Al4V TITANIUM ALLOY IN TERMS OF DEMANDED TOOL LIFE

BADANIE FUNKCJONALNOŚCI TRIBOLOGICZNEJ NARZĘDZI SKRAWAJĄCYCH POWLEKANYCH POWŁOKĄ ALTIN W OBRÓBCE STOPU TYTANU Ti6Al4V POD WZGLĘDEM WYMAGANEJ TRWAŁOŚCI NARZĘDZIA*

This paper presents a multi-factorial approach to the tool wear evolution when machining Ti6Al4V titanium alloy using high temperature resistant AlTiN coated cutting tools. Machining conditions were selected based on the technological database of machining titanium alloys in aircraft plants. The main novelty of this study is that tool wear progress within the tool life of about 20 min is assessed integrally in terms of mechanical, thermal and tribological process outputs such as cutting forces, cutting energy and cutting temperature. Moreover, the specific cutting energy (SCE), thermal softening effect and friction coefficient (CoF) were determined when recording tool wear curves. Some important research findings concerns distinguishing the three characteristic wear periods with distinctly different values of SCE and CoF. In particular, it was revealed that the formation of ceramic protective layer (CPL) on the AlTiN deposited coating influences friction and the tool wear mechanism.

Keywords: coated carbide tool, tool wear, friction, titanium alloy.

W artykule przedstawiono wieloczynnikowe podejście do ewolucji zużycia narzędzi podczas obróbki stopu tytanu Ti6Al4V przy użyciu narzędzi skrawających powlekanych, odporną na wysoką temperaturę, powłoką narzędziową AlTiN. Warunki obróbki zostały ustalone w oparciu o technologiczną bazę obróbki stopów tytanu stosowaną w przemyśle lotniczym. Główną nowością w ocenie przedstawionych badań jest to, że postęp zużycia narzędzia w okresie jego trwałości rzędu 20 minut jest oceniany integralnie, głównie pod względem mechanicznych, termicznych i trybologicznych efektów procesu skrawania, takich jak siły skrawania, energia i temperatura skrawania. Ponadto wyznaczono, adekwatne do zarejestrowanych krzywych zużycia narzędzia, wartości energii właściwej skrawania (EWS), zmiękczenia termicznego i współczynnika tarcia (WT). Niektóre ważne ustalenia badawcze dotyczą rozróżnienia trzech charakterystycznych okresów zużycia z wyraźnymi różnymi wartościami EWS i WT. W szczególności okazało się, że utworzenie ceramicznej warstwy ochronnej (CWO) na narzędziowej powłoce z AlTiN wpływa na tarcie i mechanizm zużycia narzędzia.

Słowa kluczowe: powlekane narzędzie węglkowe, zużycie narzędzia, stop tytanu.

1. Introduction

At present titanium and nickel-based alloys, also termed heat resistant superalloys (HRSAs) represent a significant percentage of construction metallic materials used in the aircraft structural and engine components [7, 9, 15]. In contrast to their attractive mechanical and physical properties their machinability rates are poor in terms of both productivity (short tool-life) and technological quality or surface integrity criteria [3, 7, 9, 11]. One of the important machining issues is appropriate cutting tool material selection in order to expose high wear resistance [3, 16], high strength and toughness, high hot hardness, chemical stability and thermal shock resistance. Some new deposition techniques such as laser heat treatments of the substrate surface [13] and nanocrystalline cemented carbides which results in distinctly stronger cutting edge [12] are proposed to enhance cutting performance.

The choice of cutting tools includes coated carbides, oxide and silicon nitride ceramic, sialon materials and coated and uncoated CBN tools [2, 7, 9]. In particular, carbide tools coated with super nitrides, such as PVD-TiAlN, AlTiN, AlCrTiN and others are widely used in the aircraft industry due to lower costs in the massive usage [2, 15, 18]. The reason is that ternary transition metal nitrides such as PVD-TiAlN, AlTiN ($Ti_{1-x}Al_xN$) coatings can effectively reduce the occurrence of abrasive wear in dry cutting but their thermo-mechanical properties and machining performance depend on many factors including mainly the stoichiometry ratio (Al/Ti ratio) [1, 2, 8, 14]. Crystal structure for TiAlN-based coatings is basically B1 but due to a high amount of aluminium ($x_{max} \sim 0.7$), the AlTiN coating contains AlN domains. As a result, the oxidation occurs at temperature of about 800°C, when for TiN coating at 600°C [1, 4]. For instance, at the ratio $x=0.54$, the coating hardness is about 34 GPa and air oxidation resistance increases up to 700°C due to the formation of a dense protective Al-rich oxide layer [10]. Earlier author's study concerning the

(*) Tekst artykułu w polskiej wersji językowej dostępny w elektronicznym wydaniu kwartalnika na stronie www.ein.org.pl

application of TiAlN coated carbide tools to the machining of nickel-chromium based superalloy Inconel 718 are presented in Ref. [5]. The main goal of this study is to document the above-mentioned properties of AlTiN in the turning of Ti6Al4V ($\alpha+\beta$) titanium alloy and support the selection of PVD-TiAlN coated tools in the aircraft plants under real production conditions taking into account all important technological requirements and physical limitations which enhance the reliability of cutting tools.

2. Experimental procedure

2.1. Workpiece material, tooling and machining conditions

The workpiece material machined was Ti6Al4V (Ti6-4) titanium alloy with the $\alpha+\beta$ microstructure and with the following chemical composition: 90%Ti, 6%Al, 4%V, max 0.25%Fe, max 0.2%O. Typically, the mechanical properties at ambient are: tensile strength of 950 MPa, compressive yield strength of 970 MPa, Young's modulus of 113.8 GPa, average hardness of 36 HRC (it is a common practice in the aerospace industry to keep the hardness below 38 HRC [17]).

Machining trials and wear tests were performed on the titanium alloy bars, using a CNC 3-axis NEF 600 lathe equipped with a FA-NUC 210i control system (Fig. 1). Rhombic cutting inserts of type CNMG 120412-UP made of sintered carbide grade KC5010 coated with PVD-Al_{0.55}Ti_{0.45}N layer of about 3 μm thickness deposited by plasma arc evaporation were used. They were clamped in ISO designation PCLNL 2525 M1 tool holder.

The following cutting parameters were selected: constant depth of cut $a_p=0.25$ mm and the feed rate $f=0.1$ mm/rev, and the variable cutting speed of 110, 130, 150 and 170 m/min. This cutting speed range was selected in the aircraft plants by highly experienced production engineers. The main task of this study was to assess the tool wear for the machining conditions specified. Hence, the experiments have to rely on the industrial procedures. The small feed rate of 0.1 mm/rev and the large tool corner radius of 1.2 mm guarantee finishing regime of the turning operations. The demanded surface roughness parameter R_a is 1.25 μm . The surface roughness was measured using laboratory contact profilometer TOPO 01P from the polish Institute of advanced manufacturing technology.

2.2. Measurement and visualization techniques

The experimental set-up is shown in Fig. 1. Three orthogonal components of the resultant cutting force (F_z , F_y and F_x) were measured using a measurement system including a Kistler 9257B piezoelectric dynamometer and a Kistler 5019 signal amplifier to amplify the generated force signals. As shown in Fig. 1a the dynamometer was clamped in the turret using a VDI clamping system. The signals were transmitted to the DAQ board using a NI 6062E A/D transducer by National Instruments. The measured data were recorded with the frequency of 2000 Hz using a Cut Pro data acquisition program. Taking into account tool wear effect the average values of the three force components were estimated using the last second of the recorded spectrum which covers about 1000 force values.

Measurements of the wear scars on the tool corner (VB_C index) and visualizations of worn tips were carried out on a Nikon SMZ 1000 stereoscopic optical microscope equipped with a CCD camera (Fig. 1b). Image processing was performed by means of an IM1000 program. Worn tool's surfaces were examined using a Hitachi S-3400N SEM scanning microscope equipped with an EDX spectral analyzer.

Measurements of the width of wear scars on the tool corner part of the flank face and visualizations of worn tips were carried out on an optical microscope equipped with a CCD camera model Nikon SMZ 1000. They were carried out in the post-process mode as shown in the left window in Fig. 1b. Image processing was performed by means of a NIS-Elements AR Nikon program. The magnification applied

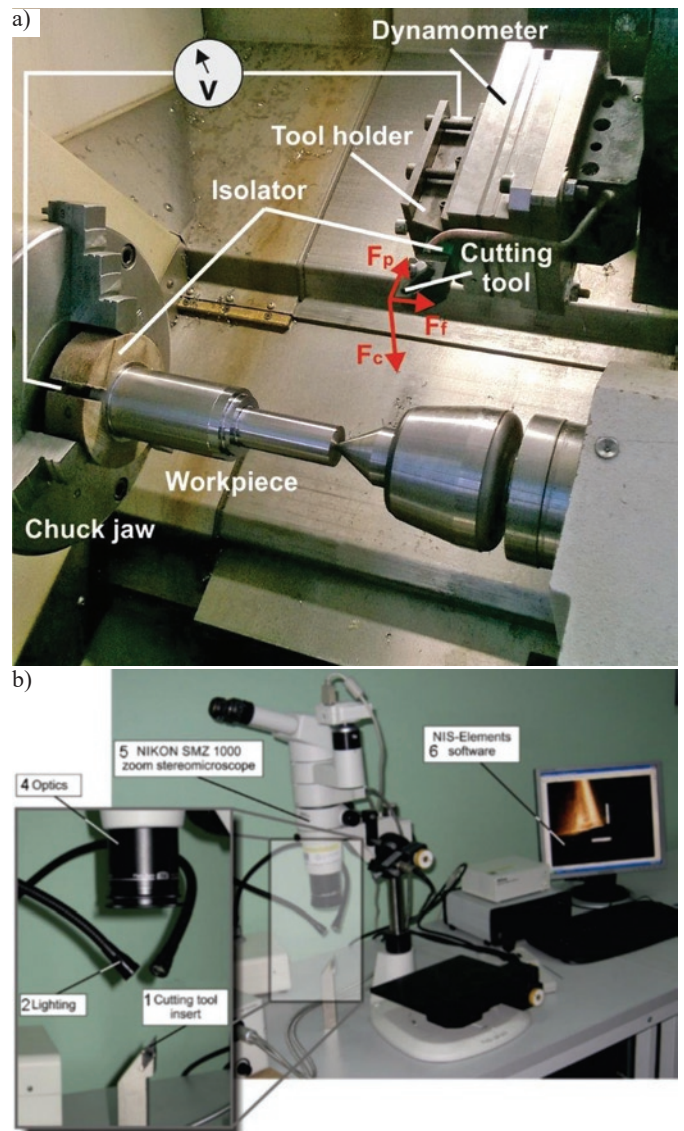


Fig. 1. Experimental set-up showing the force and natural thermocouple measurement systems (a) and measurements of tool wear scars using a CCD camera integrated with an optical microscope (b). 1-worn cutting insert, 2-lighting, 3- optical system, 4- CCD camera SMZ 1000, 5-PC with NIS-Elements program.

was 10 times under the resolution of 2560x1920 pixels. Examinations of the geometrical deteriorations of worn corners along with EDX analysis of the wear products were carried out using a SEM scanning microscope.

The cutting temperature was measured continuously during all tool wear tests using classical thermocouple methods (the measuring circuit of EMF signal is shown in Fig. 1) because a small amount of cutting fluid was supplied in order to prevent the self-ignition of the titanium chips at high temperature of above 800°C.

The changes of diffusivity for the Ti6Al4V alloy and pure aluminium versus temperature are shown in Fig. 2. It can be seen in Fig. 2 that the diffusivity of Ti6-4 alloy determined experimentally by a laser flash (LF) apparatus (model LFA-427 Netzsch) increases by about 100% when the temperature increases up to about 900°C. The methodology of the determination of thermal conductivity and diffusivity using the LF method is described in Ref. [6]. In contrast, the diffusivity of pure aluminium decreases but its values are ten times higher than for a titanium alloy. It should also be noted that

the cutting temperature should not exceed 947° due to $\alpha \rightarrow \beta$ phase transformation.

In addition, the true stress of the Ti6-4 alloy was determined using a dilatometer model Bähr 850 D/L with inductive heating and helium cooling. It was found out that the values of the true stress at the strain rate of 12.5 s^{-1} decrease from 610 MPa down to 445 MPa when temperature increases from 600°C up to 800°C. On the other hand, the hot hardness of AlTiN coating is practically constant at 1200 HV (2.6 GPa) [4]. As a result, the sliding contact conditions between the chip and the tool will be modified substantially not only due to the increase of cutting speed but also due to tool wear, and these aspects will be taken into account in Sections 3.2 and 3.3.

3. Experimental results and discussion

3.1. Relationships between tool wear and process outputs

In this study, the tool wear progresses up to the limited value of the wear width of the tool corner $VB_c=0.3 \text{ mm}$ is achieved. This tool wear index was selected due to the small depth of cut and, on the other hand, due to cutting time (tool life) demanded by aerospace plants to keep the part dimensional tolerances (KE index is equal to about $30 \mu\text{m}$ (see SEM image in Fig. 9a). It should be noted that in the aerospace industry wear curves of flank wear (FLW) vs. removed material volume (RMV) type rather than classical FLW vs. time are used.

As shown in Fig. 3, tool life corresponding to $VB_c=0.3 \text{ mm}$ is set at about 5 min, 10 min, 20 min and 50 min for the cutting speed of 110, 130, 150 and 170 m/min respectively. In this criterion, the cutting speed of 150 m/min should be recommended for aerospace practice because it guarantees the economic tool life of $T_e=20 \text{ min}$ and further analyses were performed for this cutting speed ($v_{c20}=150 \text{ m/min}$). Moreover, the cutting speed and the relevant cutting temperature should be limited due to $\alpha \rightarrow \beta$ phase transformation. As shown in Fig. 4, the cutting speed of 150 m/min is the highest cutting speed applied which fulfils this important practical criterion. For this case, the measured temperatures during wear tests (curve #3 in Fig. 4) do not exceed 750-800°C, so a safety margin of about 100-150°C is kept.

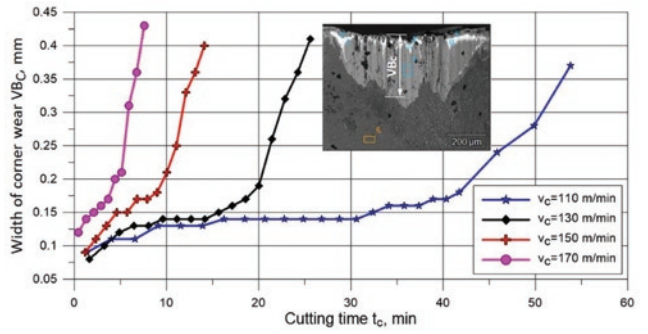


Fig. 3. A set of tool wear curves showing VB_c versus time for different cutting speeds. Constant cutting parameters - $a_p=0.25 \text{ mm}$; $f=0.1 \text{ mm}$.

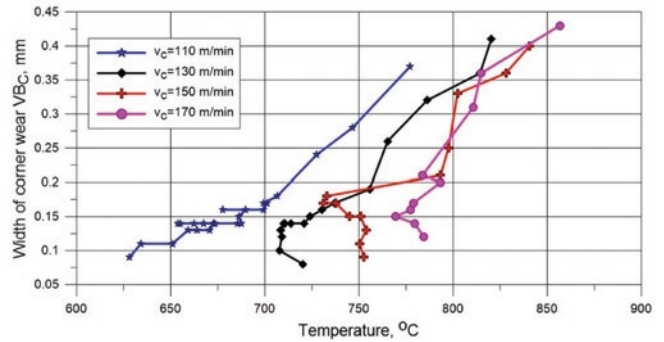


Fig. 4. Influence of tool wear on cutting temperature for variable cutting speed. Constant cutting parameters - $a_p=0.25 \text{ mm}$; $f=0.1 \text{ mm/rev}$.

increased from 0.1 to 0.2 mm (for cutting speeds of 110-150 this region is narrowed down to 0.1-0.15 mm). The average value of SCE in this tool wear region is about $3.25\text{-}3.5 \text{ GJ/m}^3$. On the other hand, the SCE increases in the next period of tool wear and for $VB_c \approx 0.3 \text{ mm}$ it is set at about 4.5 GJ/m^3 , i.e. even by 50%. Lower values of SCE were determined for the highest cutting speed of 170 m/min due to thermal softening effect (see Section 2.2). This specific tribo-phenomenon will be discussed in terms of changes of thermal diffusivity and modification of friction resulting from formation of Al_2O_3 protective layer due to the oxidation of Al in the $\text{Al}_{0.57}\text{Ti}_{0.43}\text{N}$ coating used.

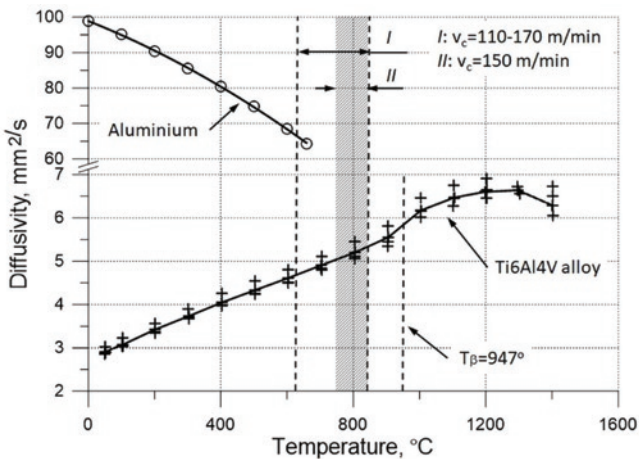


Fig. 2. The experimentally determined relationship diffusivity vs. temperature for Ti6Al4V alloy and pure aluminium.

Figs. 5 and 6 show the changes of the cutting force and equivalent values of SCE associated with tool wear evolution. The SCE (e_c) was determined as the product of the cutting force and the cutting speed ($e_c=F_c \times v_c$) [7]. As shown in Fig. 6, the SCE distributions for all tool wear evolutions are distinguished by a visible minimum which appears for cutting speeds of 110-170 m/min when the VB_c index is

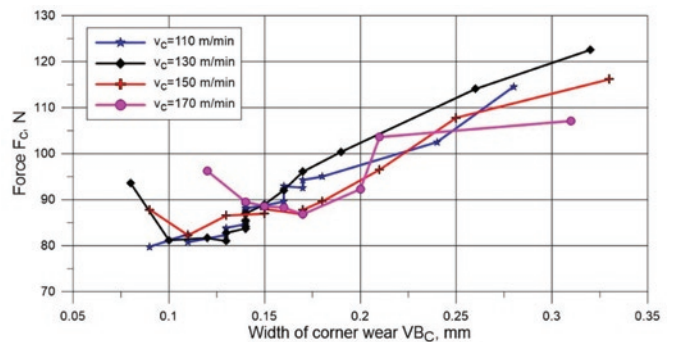


Fig. 5. The dependence of the cutting force on tool wear for different cutting speeds. Constant cutting parameters: $a_p=0.25 \text{ mm}$; $f=0.1 \text{ mm/rev}$.

3.2. Relationships between friction and wear-dependent process characteristics

Figures 7a-c present the relationships between the friction coefficient (Eqn. 1) and cutting energy (Fig. 7a), cutting temperature (Fig. 7b) and thermal diffusivity (Fig. 7c) respectively. The wear-dependent friction coefficient μ_w is calculated from the following formulae [7].

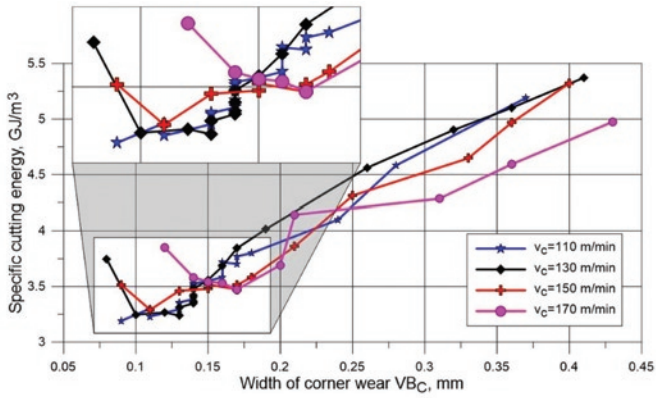


Fig. 6. The dependence of specific cutting energy on the tool wear for different cutting speeds. Constant cutting parameters: $a_p = 0.25$ mm; $f = 0.1$ mm/rev.

$$\mu_w = \frac{F_c \sin \gamma_o + F_f \cos \gamma_o}{F_c \cos \gamma_o - F_f \sin \gamma_o} \quad (1)$$

where: F_c - cutting force, F_f - feed force, γ_o - tool rake angle (it was assumed to be equal to $\gamma_o = -6^\circ$).

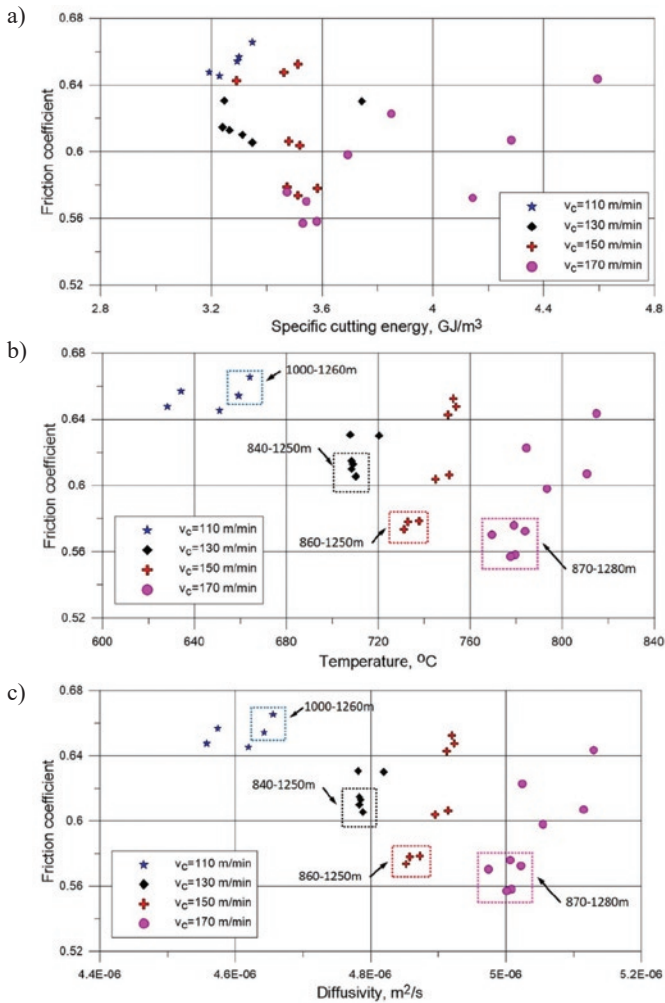


Fig. 7. The dependence of friction coefficient on specific cutting energy (a), temperature (b) and thermal diffusivity (c) for different cutting speeds and cutting length of about 1250 m. Constant cutting parameters: $a_p = 0.25$ mm; $f = 0.1$ mm/rev

It should be noted that in Eqn 1 the values of force components F_c and F_f correspond to the defined tool wear stage depending on the cutting speed applied, as shown for instance in Fig. 5 for the F_c force.

As shown in Fig. 7a, friction seems to be an energetically-based physical phenomenon and is sensitive to tool wear progress, which causes relevant increase of the SCE. In this study (Fig. 7a) the friction coefficient changes in the range of 0.56-0.66 after the cutting (sliding) distance of about 1250 m. In addition, visible differences of friction coefficient can be distinguished in terms of contact temperature (Fig. 7b) and thermal diffusivity (Fig. 7c). For comparison, the values of μ_w determined for the minimum cutting force/cutting energy (between 3.2 and 3.6 GJ/m³) documented in Figs. 6 and 7 are equal to 0.65, 0.60, 0.51 and 0.56 for the cutting speed of 110, 130, 150 and 170 m/min (Fig. 7a) respectively. From this physical criterion and conservation of the minimum energy, it is highly likely to prolong tool wear in the machining of Ti6-4 alloy up to the wear index of about $VB_C = 0.2$ mm.

3.3. Modification of tribo-contact due to tool wear evolution

The changes of the wear products produced between the AlTiN coating and the Ti 6-4 alloy as well as modification of the coating surface are determined based on EDX analysis performed in the selected points within the contact area (Fig. 8). The results of EDX analysis performed for wear products cumulated in point #1 which is localized in the chip-tool contact area close to the secondary cutting edge are specified in Tabl. 1. It can be reasoned based on this data that the content of oxygen decreases (23.2 at% vs. 17.8 at%) when the cutting speed (cutting temperature) increases from 110 to 150 m/min.

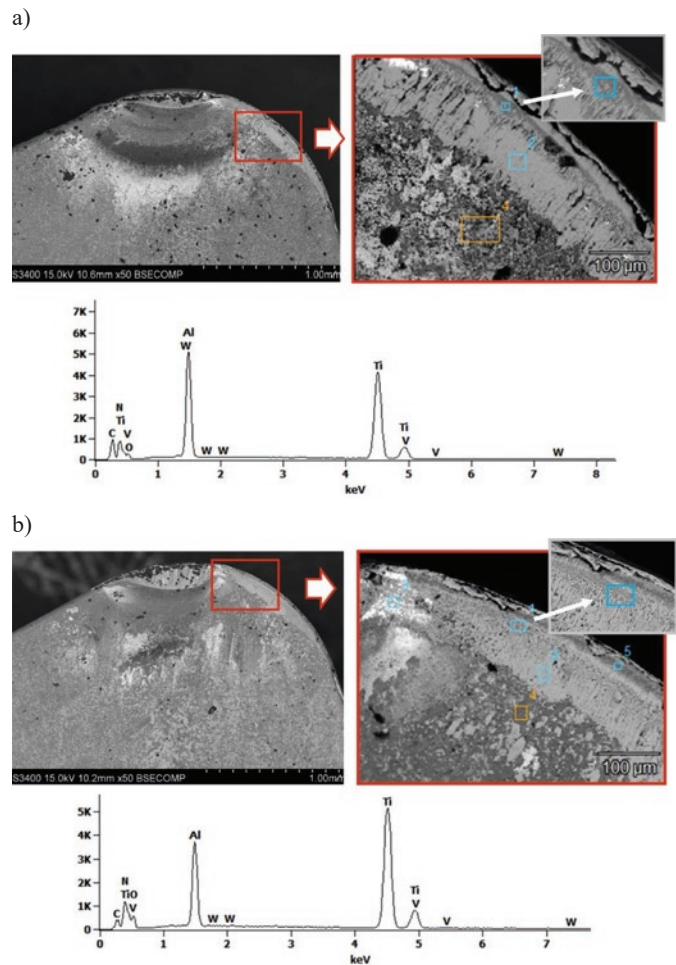


Fig. 8. SEM pictures of the fragments of worn tool corner for $vc = 110$ m/min (a) and $vc = 150$ m/min (b) and EDX spectra for point #1.

Table 1. Chemical compounds of the wear products detected in Fig. 8

V_c , m/min	Percentage	Al	Ti	V	O
110	wt%	19.6	61.0	1.8	17.4S
	at%	23.2	40.7	1.1	34.9
150	wt %	13.5	71.6	2.8	12.0S
	at%	17.8	53.4	1.9	26.8

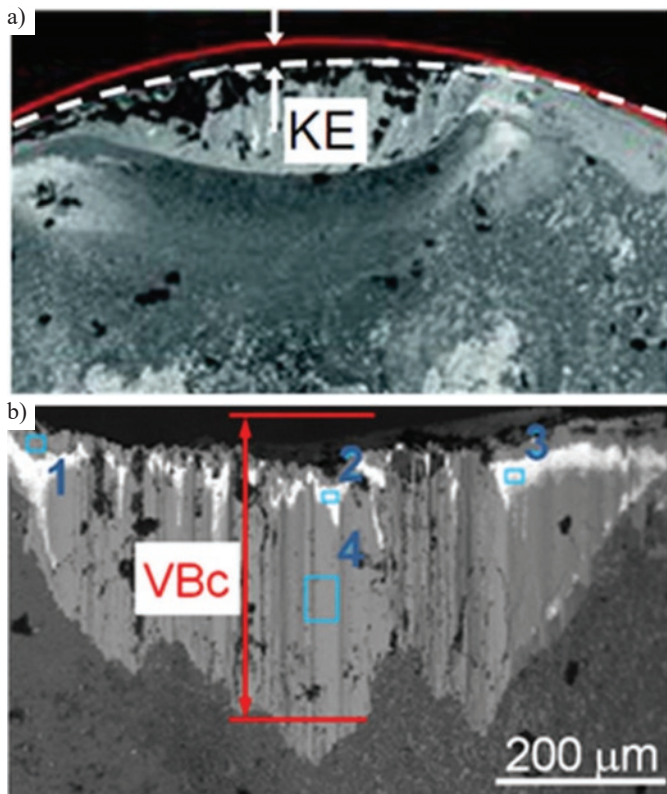


Fig. 9. SEM pictures of worn tool corner with KE (a) and VBC (b) indexes.

This means that at higher cutting speeds and at the temperature of about 750°C (Fig. 8a) the oxidation process of the AlTiN coating is more intensive. On the other hand, the content of Ti, whose diffusiv-

ity is approximately 10 times lower than for Al (see Fig. 3), increases from 40.7 at% up to 53.4 at%.

Figure 9b shows the SEM image of worn corner area after 14 min of wear evolution. In all points #1-4 within the worn area the content of Al is very low (5-10 at%) but the Ti content is very high even as high as 85 at% in points # 2 and 4. In point #6 which is localized on the unworn AlTiN coating the contents of Al and Ti are equal to 58 and 41.2 at% respectively (the rest are vanadium V and iron Fe).

4. Conclusions

1. This study clearly explained the influence of tool wear on friction modification resulting from thermal effects including thermal softening, increase of thermal diffusivity and the formation of protective ceramic layer.
2. Tool wear is strongly associated with changes of SCE and thermal softening effect depending on the cutting speed. Moreover, the minimum energy consumption region is detected when tool wear index VBC approaches 0.1-0.2 mm depending on the cutting speed used. Cutting temperatures suggest that at this period of tool wear the onset of oxidation of Al in AlTiN coating occurs.
3. The choice of tool life in the machining of Ti6-4 alloy should be based not only on technological but also physical criteria such as contact temperature, material softening effect or thermal diffusivity indicating the formation of ceramic protective layer (CPL) on the deposited coating. In general, cutting speeds higher than 150 m/min (equivalent temperature of 750-800°C) are necessary to produce CPL on the $Al_{0.55}Ti_{0.45}N$ coating.
4. Future studies should be focussed on the formation of Al_2O_3 protective layer for the specific machining conditions recommended in aerospace industry in terms of the $Al_{1-x}Ti_xN$ stoichiometry.

Acknowledgments

This research is supported by the European Regional Development Fund and the National Centre for Research and Development Poland (NCBR)- Grant No. INNOLOT/1/7/NCBR/2013 (2013-2018).

References

1. Alling B, Ruban A, Karimi A, Peil O, Simak S, Hultman S, Abrikosov L. Mixing and decomposition thermodynamics of c-Ti1-xAlxN first-principles calculation. *Physical Review B* 2009; 75 (045123): 1-13.
2. Bouzakis K D, Michailidis N, Skordaris G, Bouzakis E, Bierman D M, Saoubi R. Cutting with coated tools: coating technologies, characterization methods and performance optimization. *CIRP Annals-Manufacturing Technology* 2012; 61: 587-609, <https://doi.org/10.1016/j.cirp.2012.05.006>.
3. Cantero J L, Díaz-Álvarez J, Miguélez M H, Marín N C. Analysis of tool wear patterns in finishing turning of Inconel 718. *Wear* 2013; 297: 885-894, <https://doi.org/10.1016/j.wear.2012.11.004>.
4. Chim Y C, Ding X Z, Zeng X T, Zhang S. Oxidation resistance of TiN, CrN, TiAlN and CrAlN coatings deposited by lateral rotating cathodic arc. *Thin Solid Films* 2009; 517: 4845-4849, <https://doi.org/10.1016/j.tsf.2009.03.038>.
5. Grzesik W, Niesłony P, Habrat W. Investigation of tool wear in the turning of Inconel 718 superalloy in terms of process performance and productivity enhancement. *Tribology International* 2018; 118: 337-346, <https://doi.org/10.1016/j.triboint.2017.10.005>.
6. Grzesik W, Niesłony P, Laskowski P. Determination of material constitutive laws for Inconel 718 superalloy under different strain rates and working conditions. *Journal of Materials Engineering and Performance* 2017; 26: 5705-5714, <https://doi.org/10.1007/s11665-017-3017-8>.
7. Grzesik W. *Advanced machining processes of metallic materials*. New York: Elsevier 2017.
8. Kajzer W, Jaworska J, Jelonek K, Szewczenko J, Kajzer A, Nowińska K, Hercog A, Kaczmarek M, Kasperczyk J. Corrosion resistance of Ti6Al4V alloy coated with caprolactone-based biodegradable polymeric coatings. *Eksploatacja i Niezawodność – Maintenance and Reliability* 2018; 20(1): 30-38, <https://doi.org/10.17531/ein.2018.1.5>.

9. Klocke F. Manufacturing Processes 1. Berlin: Springer, 2011, <https://doi.org/10.1007/978-3-642-11979-8>.
10. Koller C M, Hollerweger R, Sabitzer C, Rachbauer R, Kolozvari S, Paulisch J, Mayrhofer P H. Thermal stability and oxidation resistance of arc evaporated TiAlN, TaAlN, TiAlTaN, and TiAlN/TaAlN coatings. Surface and Coatings Technology 2014; 259: 599-607, <https://doi.org/10.1016/j.surfcoat.2014.10.024>.
11. Królczyk G, Gajek M, Legutko S. Predicting the tool life in the dry machining of duplex stainless steel. Eksploatacja i Niezawodność – Maintenance and Reliability 2013; 15 (1): 62–65.
12. Kupczyk M. Cutting edges with high hardness made of nanocrystalline cemented carbides. International Journal of Refractory Metals and Hard Materials 2015; 49 (1): 249–255, <https://doi.org/10.1016/j.ijrmhm.2014.07.041>.
13. Kupczyk M, Jozwiak K, Cieszkowski P, Libuda P. Influence of laser heating on adhesion of CVD coatings to cutting edges. Surface and Coatings Technology 2007; 201 (9–11): 5153–5156, <https://doi.org/10.1016/j.surfcoat.2006.07.155>.
14. Kutschej K, Mayrhofer P H, Kathrein M, Polcik P, Tessadri, Mitterer C. Structure, mechanical and tribological properties of sputtered Ti1-xAlxN coatings with 0.5x0.75. Surface and Coatings Technology 2005; 200: 2358-2365, <https://doi.org/10.1016/j.surfcoat.2004.12.008>.
15. M'Saoubi R, Axinte D, Soo SI, Nobel Ch, Attia H, Kappmeyer G, Engin S, Sim WM. High performance cutting of advanced aerospace alloys and composite materials, CIRP Annals- Manufacturing Technology 2015; 64: 557-580.
16. Maruda R, Krolczyk G, Feldshtein E, Nieslony P, Tyliczszak B, Pusavec F. Tool wear characterizations in finish turning of AISI 1045 carbon steel for MQCL conditions. Wear 2017; 372–373: 54-67, <https://doi.org/10.1016/j.wear.2016.12.006>.
17. Material Properties Database- MPDB v. 8.37, www.jahm.com.
18. Zębala W, Słodki B, Struzikiewicz G. Productivity and reliability improvement in turning Inconel 718 alloy – case study. Eksploatacja i Niezawodność – Maintenance and Reliability 2013; 15(4): 421-426.

Wit GRZESIK**Piotr NIESŁONY**

Faculty of Mechanical Engineering
Opole University of Technology
ul. Proszkowska 76, 45-758 Opole, Poland

Witold HABRAT

Faculty of Mechanical Engineering and Aeronautics
Rzeszów University of Technology
al. Powstańców Warszawy 12, 35-959 Rzeszów, Poland

E-mails: w.grzesik@po.opole.pl, p.nieslony@po.opole.pl,
witekhab@prz.edu.pl
